DMD Fast Forward. Published on April 25, 2013 as doi:10.1124/dmd.113.051722

DMD/2013/051722

Inhibition of CYP2C19 and CYP3A4 by Omeprazole Metabolites and their Contribution to Drug-Drug Interactions

Yoshiyuki Shirasaka and Jennifer E. Sager, Justin D. Lutz, Connie Davis and Nina Isoherranen

Department of Pharmaceutics, School of Pharmacy (Y.S., J.E.S., J.D.L., N.I.), and Division of Nephrology, Department of Medicine, School of Medicine (C.D.) University of Washington, Seattle, Washington, USA, and Faculty of Pharmacy, Institute of Medical, Pharmaceutical and Health Sciences, Kanazawa University, Kakuma-machi, Kanazawa, Japan (Y.S.)

Running Title:

CYP2C19 and CYP3A4 Inhibition by Omeprazole Metabolites

Address Correspondence to:

Nina Isoherranen, Ph.D.

Department of Pharmaceutics, School of Pharmacy, University of Washington, H272 Health Sciences Building, Box 357610, University of Washington, Seattle, WA 98195-7610, USA

Tel.: 206-543-2517; Fax: 206-543-3204

E-mail: ni2@u.washington.edu

The Number of

Text Pages: 36

Tables: 3

Figures: 5

References: 39

The number of words in

Abstract: 245

Introduction: 708

Discussion: 1495

Abbreviations:

AUC, Area under the plasma concentration-time curve; C_{max}, maximum concentration in plasma;

C-OMP, carboxyomeprazole; DDI, drug-drug interaction; DM-OMP, 5'-O-desmethylomeprazole; EMA, European Medicines Agency; FDA, US Food and Drug Administration; $f_{u,\,p,}$ fraction of drug unbound in plasma; $f_{u,mic,}$ fraction of drug unbound in microsomes; OH-OMP, 5-hydroxyomeprazole; HLM, human liver microsome; [I], inhibitor or inactivator concentration; IC_{50}, inhibitor concentration that results in half-maximal P450 inhibition; k_{deg}, rate constant for *in vivo* P450 degradation; K_i, inhibition constant for P450 inhibition; K_I, inhibitor concentration that results in half-maximal rate of P450 inactivation; K_m, substrate concentration the results in half-maximal P450 activity; k_{inact}, first-order rate constant for P450 inactivation; λ, apparent inactivation rate at a given inhibitor concentration; MBI, mechanism-based inhibition or inhibitor; OMP, omeprazole; OMP-S, omeprazole sulfone; P450, cytochrome P450; PPI, proton pump inhibitor.

DMD Fast Forward. Published on April 25, 2013 as DOI: 10.1124/dmd.113.051722
This article has not been copyedited and formatted. The final version may differ from this version.

Abstract

The aim of this study was to evaluate the contribution of metabolites to drug-drug interactions (DDI) using the inhibition of CYP2C19 and CYP3A4 by omeprazole and its metabolites as a model. Of the metabolites identified in vivo, 5-hydroxyomeprazole, 5'-O-desmethylomeprazole, omeprazole sulfone and carboxyomeprazole had an $AUC_m/AUC_p \geq 0.25$ when either total or unbound concentrations were measured following a single 20 mg dose of omeprazole in a cocktail. All of the metabolites inhibited CYP2C19 and CYP3A4 reversibly. In addition omeprazole, omeprazole sulfone and 5'-O-desmethylomeprazole were mechanism-based inhibitors (MBI) of CYP2C19 while omeprazole and 5'-O-desmethylomeprazole were found to be MBIs of CYP3A4. Reversible $[I]/K_i$ ratios and irreversible λ/k_{deg} ratios were used to evaluate whether characterization of the metabolites affected DDI risk assessment. Identifying omeprazole as an MBI of both CYP2C19 and CYP3A4 was the most important factor in DDI risk assessment. Consideration of reversible inhibition by omeprazole and its metabolites would not identify DDI risk with CYP3A4, and with CYP2C19 reversible inhibition values would only identify DDI risk if the metabolites are included in the assessment. Based on inactivation data, CYP2C19 and CYP3A4 inactivation by omeprazole would be sufficient to identify risk, but metabolites were predicted to contribute 30-63% to the in vivo hepatic interactions. Hence, consideration of metabolites may be important in quantitative predictions of in vivo DDIs. The results of this study show that while metabolites contribute to in vivo DDIs their relative abundance in circulation or logP values do not predict their contribution to in vivo DDI risk.

Introduction

Inhibitory drug-drug interactions (DDIs) can result in significant increases in the area under the plasma concentration-time curve (AUC) of an object drug by reducing systemic clearance or increasing bioavailability. Due to potential adverse effects exacerbated by inhibitory DDIs, they are of serious concern in drug development. Consequently, the ability to reliably identify potential in vivo inhibitors and predict the magnitude of DDIs from in vitro data is necessary. The recommended methods for performing pre-clinical risk assessment and quantitative DDI predictions have been outlined by the US Food and Drug Administration (FDA) (http://www.fda.gov/downloads/Drugs/GuidanceComplianceRegulatoryInformation/Guidances/ucm292362.pdf) and the European Medicines Agency (EMA) (http://www.ema.europa.eu/docs/en_GB/document_library/Scientific_guideline/2012/07/WC500129606.pdf). Included in the most recent guidances is the recommendation that metabolites be considered in DDI risk assessment if metabolite AUC is greater than 25% of the parent AUC ($AUC_m/AUC_p \geq 0.25$). The EMA further emphasizes that, if available, unbound concentrations should be used to determine relative exposures and that metabolites should also represent >10% of total drug related material.

Using retrospective data, it has been recognized that many P450 inhibitors possess circulating metabolites (Isoherranen et al., 2009), and that inclusion of the metabolites in risk analysis can, in some cases, prevent false negative predictions (Yeung et al., 2011). However, prospective studies aimed at understanding the importance of metabolites in DDI risk assessment are lacking, and the overall role of inhibitory metabolites in clinical DDIs and DDI predictions is still not well characterized. The relatively sparse data regarding inhibition potency of circulating metabolites (Yeung et al., 2011) has left the quantitative importance of metabolites in risk

assessment controversial (Yu et al. 2012). In addition, very few studies have evaluated the importance of metabolites in irreversible interactions, despite the fact that most of clinically important mechanism-based inhibitors (MBI) possess circulating metabolites (VandenBrink and Isoherranen, 2010). Hence more studies are needed to determine the role of circulating metabolites in reversible and irreversible P450 inhibition, and to evaluate the correlation between abundance of metabolites in circulation and their contribution to inhibitory DDIs.

Omeprazole (OMP), which is metabolized by CYP2C19 and CYP3A4 (Andersson et al., 1994) is also an in vivo inhibitor of these two enzymes (Yu et al., 2001; Angiolillo et al., 2011; Funck-Brentano et al., 1997; Soons et al., 1991). OMP has been found to reversibly inhibit both CYP2C19 and CYP3A4 in vitro and recent investigations have shown that OMP is also an irreversible inhibitor of CYP2C19 (Ogilvie et al., 2011 Boulenc et al., 2012). While in vivo DDIs with CYP2C19 substrates following OMP administration can largely be explained by CYP2C19 inactivation, the mechanisms of in vivo CYP3A4 interactions remain unexplained. It has been suggested that OMP metabolites may contribute to CYP2C19 inhibition (Ogilvie et al., 2011) but the metabolites have not been incorporated into DDI predictions and their circulating concentrations are not well characterized. In addition, it is possible that OMP metabolites are responsible for the in vivo CYP3A4 inhibition observed (Soons et al., 1991). Since OMP is a weak-to-moderate inhibitor of CYP2C19 and CYP3A4 in vivo, inclusion of metabolites in DDI risk assessment may change the risk categorization significantly. Two of the omeprazole metabolites, 5-hydroxyomeprazole (OH-OMP) and omeprazole sulfone (OMP-S), are known to be present in plasma following omeprazole administration, and OMP-S shows elimination rate-limited kinetics in vivo (Regårdh et al., 1990). While OMP-S inhibits both CYP2C19 and CYP3A4 reversibly in vitro, its contribution to in vivo CYP2C19 and CYP3A4 inhibition was

predicted to be insignificant and inclusion of OMP-S to DDI risk assessment did not identify the in vivo CYP3A4 inhibition risk by OMP (Yeung et al., 2011). As such, OMP DDIs are insufficiently characterized and further investigations are required to determine the potential contribution of the other circulating OMP metabolites to in vivo CYP2C19 and CYP3A4 interactions.

The aim of this study was to systematically evaluate the contribution of OMP metabolites to inhibitory DDIs observed with CYP2C19 and CYP3A4 after OMP administration. The circulating metabolites of OMP were identified in vivo in 9 healthy human volunteers following a single 20 mg dose of OMP, and those metabolites meeting the recommended plasma exposure cutoff for DDI testing were evaluated in vitro for CYP2C19 and CYP3A4 inhibition. The obtained data was then used to assess the relative importance of the metabolites in in vivo DDIs and in DDI risk assessment.

Materials and Methods

Chemicals and Reagents: Human liver microsomes (HLM) from seven donors were obtained from the University of Washington Human Liver Bank maintained by the School of Pharmacy, University of Washington (Seattle, WA). HLMs were prepared using standard ultracentrifugation methods and were pooled prior to use. All donors were CYP2C19 extensive metabolizers and CYP3A5 non-expressers. OMP, OH-OMP, 5'-O-desmethylomeprazole (DM-OMP), OMP-S, carboxyomeprazole (C-OMP), omeprazole sulphone N-oxide, omeprazole sulfide, omeprazole N-oxide, dextrorphan glucuronide and 4-hydroxymephenytoin-d_3 were purchased from Toronto Research Chemicals (Ontario, Canada). (S)-mephenytoin, sulfatase from *Aerobacter aerogenes,* β-glucuronidase from *Escherichia coli,* and 4-nitrocatechol sulfate dipotassium salt were purchased from Sigma-Aldrich (St. Louis, MO). Midazolam, 1'-hydroxymidazolam and α-hydroxymidazolam-d_4 were purchased from Cerilliant (Round Rock, TX). Optima grade acetonitrile and water were purchased from Fisher Scientific. All other chemicals and general reagents were of analytical grade or better and were obtained from various commercial sources such as Invitrogen (Carlsbad, CA) or Applied Biosystems (Foster City, CA).

Clinical Study: The study protocol was approved by the University of Washington Institutional Review Board, and the study was registered at www.clinicaltrials.gov (NCT01361217). Plasma samples were obtained from the control day (no inhibitor) of the study. Nine subjects (5 men and 4 women) participating in a cocktail study received a validated cocktail (Ryu et al, 2007) of 100 mg caffeine, 2 mg midazolam, 30 mg dextromethorphan and 20 mg omeprazole (delayed release formulation) orally with 250 mL of water. It has been previously shown that the individual drugs in the cocktail do not affect the disposition of each other following a single dose

administration (Ryu et al, 2007). All participants were CYP3A5 non-expressers and CYP2C19 extensive metabolizers based on genotype analysis. Blood was collected at 0, 0.25, 0.5, 0.75, 1, 1.5, 2, 3, 4, 6, 8, and 12 hours following dosing, plasma separated from blood by centrifugation and stored at -80°C until analysis.

To establish the importance of conjugation reactions in the elimination of omeprazole metabolites an aliquot of each plasma sample was treated with either β-glucuronidase from *Escherichia coli* or sulfatase from *Aerobacter aerogenes*. For β-glucuronidase treatment the enzyme was diluted in 100mM potassium phosphate buffer, pH 6.8 to a concentration of 500 units/mL. 50µL was then added to an equal volume of plasma and the samples were incubated in the dark at 37°C overnight. Deconjugation of dextrorphan glucuronide in blank plasma was used as a positive control. For sulfatase treatment, the enzyme was diluted in 100mM potassium phosphate buffer, pH 7.1 to a concentration of 1 unit/mL. 50µL was added to an equal volume of plasma and the samples were incubated in the dark at 37°C overnight. Deconjugation of 4-nitrocatechol sulfate dipotassium salt in plasma was used as a positive control. Deconjugation to 4- nitrocatechol was determined by measuring the absorbance at 515 nM. Negative control samples containing 50µL plasma and 50µL of the respective buffer were also incubated in the dark at 37°C overnight. 50µL of reaction mix was quenched in 100µL 1:3 acetonitrile:methanol containing 100nM omeprazole-d_3 internal standard. OMP, DM-OMP, OMP-S, C-OMP and OH-OMP were measured using LC/MS/MS as described below. The relative importance of the conjugates in plasma was determined by subtracting the concentrations of each analyte in control plasma from concentrations of the analytes in treated plasma.

Analysis of Omeprazole and Its Metabolites in Human Plasma: Plasma samples (67µL) were

DMD Fast Forward. Published on April 25, 2013 as DOI: 10.1124/dmd.113.051722
This article has not been copyedited and formatted. The final version may differ from this version.

protein precipitated with 3:1 acetonitrile:methanol (133 µL) containing 100 nM d_3-omeprazole, centrifuged twice at 3000 *g* for 15 min, and the supernatant was transferred to clean plates between each spin. Samples were analyzed by LC-MS as described below. The area under plasma concentration time curve from time 0 to infinity ($AUC_{0-\infty}$) was calculated by the trapezoidal method using noncompartmental analysis and Phoenix software (Pharsight, Mountainview, CA).

LC/MS/MS Analysis of omeprazole and its metabolites in human plasma and 1'-hydroxymidazolam and 4-hydroxymephenytoin in human liver microsome incubations: The concentrations of analytes in plasma samples and in incubations were determined using a liquid chromatography-tandem mass spectrometry (LC/MS/MS) system consisting of a AB-Sciex API 3200® triple quadrupole mass spectrometer (AB Sciex, Foster City, CA) coupled with a LC-20AD® ultra fast liquid chromatography (UFLC) system (Shimadzu Co., Kyoto, Japan). An Agilent ZORBAX XDB-C18 column (5µm, 2.1×50 mm) was used to separate 4-hydroxymephenytoin and 1'-hydroxymidazolam and a Thermo Hypersil Gold 100 x 2.1 mm, 1.9 µm column (West Palm Beach, FL) was used to separate OMP, OH-OMP, DM-OMP, OMP-S, C-OMP, omeprazole N-oxide, omeprazole sulfone N-oxide, and omeprazole sulfide. The Turbo Ion Spray interface was operated in positive ion mode. A mobile phase of 0.1% aqueous formic acid (A) and acetonitrile (B) was used and the injection volume was 10 µL. For the quantitative determination of 4-hydroxymephenytoin, a flow rate of 0.3 mL/min was used with a gradient elution starting from 5% B increased to 70% B by 3.0 min, then increased to 95% B by 3.1 min and kept at 95% B until 5.0 min, then returned to initial conditions by 7 min. The retention time of 4-hydroxymephenytoin was 4.0 min and the mass transitions (*m/z)* were 235.157→150.200 and 238.157→150.200 for 4-hydroxymephenytoin and d_3-4-hydroxymephenytoin, respectively.

For the quantitative determination of 1'-hydroxymidazolam, OMP, OH-OMP, DM-OMP, OMP-S, C-OMP, omeprazole sulfone N-oxide, omeprazole sulfide, omeprazole N-oxide, and dextrorphan glucuronide a flow rate of 0.4 mL/min was used with gradient elution with initial 10% of B increased to 90% B by 3.5 min and kept at 90% B until 5 min, then returned to initial conditions by 7 min. The mass transitions (*m/z)* and retention times were as follows: 342.107→324, 2.40 min (1'-hydroxymidazolam), 346.1→328, 2.87 min (α-hydroxymidazolam-d_3), 346.1→198, 2.88 min (OMP), 349.1→198.1, 2.87 min (d_3-OMP), 362→150, 2.99 min (omeprazole N-oxide), 362→214.10, 2.70 min (OH-OMP), 332.1→198.1, 2.48 min (DM-OMP), 362→150, 3.21 min (OMP-S), 376→149.2, 2.67 min (C-OMP), 330.2→182, 3.05 min (omeprazole sulfide), 378→166, 3.12 min (omeprazole sulfone N-oxide) and 434→258, 2.16 min (dextrorphan glucuronide).

Analyst software version 1.4 (AB Sciex, Foster City, CA) was used for data analysis. The day-to-day coefficient of variation percentage for all analytes was <15%. The limit of quantification for 1'-hydroxymidazolam, OMP, OH-OMP, DM-OMP, OMP-S and C-OMP was 1nM and the limit of quantification for 4-hydroxymephenytoin was 50 nM.

Determination of Protein Binding of Omeprazole and Its Metabolites and LogP Calculations: OMP and its metabolites were added to 0.1 mg/mL HLM, 1.0 mg/mL HLM or blank plasma to yield a final concentration of 1 µM (plasma) or 10 µM (HLM) and protein binding was determined using ultracentrifugation as described previously (Templeton et al., 2008; Lutz and Isoherranen, 2012). Samples were aliquoted into ultracentrifuge tubes (Beckman 343775) and incubated at 37°C for 90 min or spun at 435,000 g at 37°C for 90 minutes using a Sorval Discovery M150 SE ultracentrifuge with a Thermo Scientific S100-AT3 rotor (Waltham, MA). The supernatant or the incubated sample was added to an equal volume

DMD Fast Forward. Published on April 25, 2013 as DOI: 10.1124/dmd.113.051722
This article has not been copyedited and formatted. The final version may differ from this version.

of acetonitrile containing 100 nM d_3-OMP and samples were centrifuged at 3,000 *g* for 15 min at 4°C. HLM supernatant was transferred to a clean plate while plasma supernatant was centrifuged a second time prior to analysis. The fraction unbound (f_u) was calculated as the ratio of inhibitor concentration with or without ultracentrifugation. Calculated XlogP3 values were generated using Virtual Computational Chemistry Laboratory (vcclab.org).

Inhibition Experiments in HLMs to Determine IC_{50} Values: Experiments were conducted at (S)-mephenytoin and midazolam concentrations of 20 μM and 1 μM, respectively (5-fold below reported K_m values). Incubations were performed in solutions containing 100 mM potassium phosphate buffer (KPi, pH 7.4) and final incubation volumes were 100 μL and 150 μL for CYP2C19 and CYP3A4 assays, respectively. OMP or its metabolites (≥7 concentrations between 0.5 and 1000 μM), HLM (0.1 mg/mL) and substrate were preincubated for 10 minutes at 37°C before reactions were initiated by adding NADPH (1 mM, final concentration). Reactions were terminated after 20 minutes ((S)-mephenytoin) or 4 minutes (midazolam) by adding an equal volume of ice-cold acetonitrile containing 100 nM internal standard. All experiments were carried out in triplicate. IC_{50} values were estimated by fitting Equation 1 to the data using nonlinear least-squares analysis in GraphPad Prism (Synergy Software, Reading, PA) (Peng et al 2012) and the MULTI program (Yamaoka et al., 1981). Data are given as the mean of values obtained in at least three experiments with standard deviation.

$$\%\ \text{of control activity} = \frac{100 \times IC_{50}}{IC_{50} + [\mathrm{I}]} \qquad (1)$$

***IC_{50}*-Shift Experiments in HLMs for Mechanism-Based Inhibition:** Incubations were performed in solutions containing 100 mM potassium phosphate buffer (KPi, pH 7.4). For CYP2C19 studies, OMP and its metabolites (7 concentrations between 0.01 and 100 μM) were incubated with 0.1 mg/mL HLM in 100 μL KPi buffer at 37°C for 30 minutes in the presence or

DMD Fast Forward. Published on April 25, 2013 as DOI: 10.1124/dmd.113.051722
This article has not been copyedited and formatted. The final version may differ from this version.

absence of NADPH before (S)-mephenytoin (20 μM) or (S)-mephenytoin + NADPH were added. For CYP3A4 studies, OMP and its metabolites (7 concentrations between 0.1 and 1000 μM) were incubated in 150 μL KPi buffer with 0.1 mg/mL HLM at 37°C for 30 minutes in the presence or absence of NADPH before midazolam (1 μM) or midazolam + NADPH were added. Reactions were terminated after 15 min ((S)-mephenytoin) or 3 min (midazolam) by adding an equal volume of acetonitrile containing 100 nM internal standard. The magnitude of the IC_{50} shift was determined from the ratio of the IC_{50} values after preincubation with and without NADPH. A shift ≥1.5 was considered to indicate irreversible inhibitory potential (Berry and Zhao, 2008; Grimm et al., 2009). Data are given as the mean of values obtained in triplicate experiments with standard deviation.

Inactivation Experiments in HLMs and CYP3A4 supersomes to Determine K_I and k_{inact} Values*:* Mechanism-based inhibition was evaluated using the dilution method previously described (Waley et al., 1985). Incubations were performed in solutions containing 100 mM potassium phosphate buffer (KPi, pH 7.4). For CYP2C19 studies, HLM (1 mg/mL) were incubated at 37°C with OMP, DM-OMP or OMP-S (8 concentrations between 0.1 and 300 μM) and NADPH (1 mM). For CYP3A4 studies, HLM (1 mg/mL) were incubated at 37°C with OMP or DM-OMP (7 concentrations between 1 and 500 μM) and NADPH (1 mM). At four designated time points, 10 μL aliquots were diluted 10-fold into activity assays containing a saturating concentration of (S)-mephenytoin (200 μM) or midazolam (30 μM) (approximately 5-fold higher than substrate K_m) and NADPH (1 mM final concentration). Reactions were allowed to proceed for 15 min ((S)-mephenytoin) or 3 min (midazolam) at 37°C. Inactivation experiments using CYP3A4 supersomes (b5 and P450 reductase coexpressed) were performed similarly to those described above with 5 pmoles CYP3A4. All reactions were terminated by

DMD Fast Forward. Published on April 25, 2013 as DOI: 10.1124/dmd.113.051722
This article has not been copyedited and formatted. The final version may differ from this version.

adding an equal volume of acetonitrile containing 100 nM internal standard. Inactivation kinetic parameters (k_{inact} and K_I values) were determined by nonlinear least-squares analysis (Graphpad Prism or the MULTI program) by fitting equation 2 to the data:

$$\lambda = \frac{k_{inact} \cdot [I]}{K_I + [I]} \quad (2)$$

where the λ is the apparent first-order rate constant of inactivation at a given inhibitor concentration, k_{inact} is the maximum inactivation rate (min^{-1}), and K_I is the inactivator concentration when the rate of inactivation reaches half of k_{inact} (μM). Data are given as the mean of values obtained in triplicate experiments with standard deviation (SD).

DDI Risk Assessment: The DDI risk was determined by calculating the [I]/K_i ([I]/IC_{50}) and λ/k_{deg} ratios for reversible and irreversible inhibition, respectively (Fujioka et al., 2012). In the present study, IC_{50} values can be regarded as equal to the K_i values because substrate concentrations were well below the relevant K_m values. The value for in vivo λ was predicted using equation 2 by substituting the in vivo inhibitor concentrations (C_{max}) for [I]. The values used for $k_{deg,CYP}$ for CYP2C19, hepatic CYP3A4 and intestinal CYP3A4 were 0.00045 min^{-1}, 0.00032 min^{-1} and 0.00048 min^{-1}, respectively (Nishiya et al., 2009; Ogilvie et al., 2011; Fahmi et al., 2008). The FDA recommends using total C_{max} values for [I] while the EMA recommends using unbound C_{max} values, hence DDI risk was predicted using both values. Unbound K_i and K_I values were used in all calculations. Intestinal CYP3A4 inhibition was included in the risk assessment using an $[I]_g$ of Dose/250mL as the worst case scenario according to the FDA guidance. [I]/K_i ratios ≥ 0.1 and 0.02 were considered as indications of DDI risk, in accordance with the FDA and EMA guidances, respectively. DDI risk due to irreversible inhibition was considered as λ/k_{deg} values ≥ 0.1 and 0.25, as stated in the FDA and EMA guidances, respectively. The relative contribution of the metabolites was calculated as a fraction of the total predicted

inhibition as described previously (Templeton et al., 2008).

Results

Identification of Significant OMP Metabolites: Plasma was collected from 9 subjects following a 20 mg single oral dose of OMP in a validated cocktail. The plasma samples were first analysed to identify all OMP related metabolites. A total of seven metabolites were identified (data not shown), and several additional OMP related compounds including conjugates of the metabolites were detected but the identity of all of these minor metabolites could not be determined. The circulating concentrations of OMP, OH-OMP, DM-OMP, OMP-S, C-OMP, omeprazole N-oxide, omeprazole sulfide and omeprazole sulfone N-oxide were further measured using LC-MS/MS. The C_{max} value of OMP was 660 nM. Omeprazole-N-oxide was detectable in 1-4 samples of each subject (18% of all samples), omeprazole-sufide was detectable in 2-6 samples per subject (29% of all samples) and omeprazole-sulfone N-oxide was detectable in 1-6 samples per subject (36% of all samples). However, all of the concentrations were below the lower limit of quantification of these compounds (LLOQs were 63 nM for OMP N-oxide, 16 nM for OMP sulfide and 31 nM for OMP sulfone N-oxide) making them minor circulating metabolites. The mean plasma concentration-time profiles of OMP, OH-OMP, DM-OMP, OMP-S and C-OMP are shown in Fig. 1, and the C_{max}, $AUC_{0-\infty}$ and unbound fraction in plasma ($f_{u,p}$) are listed in Table 1. Treatment of plasma samples with β-glucuronidase and sulfatase led to an increase in DM-OMP plasma concentrations, but based on quantification of the conjugated fraction these conjugates were quantitatively minor. Similarly, deconjugation increased plasma concentrations of C-OMP and OH-OMP in some samples, but only slightly (<20%) demonstrating that conjugates of these compounds are not quantitatively important in circulation. The total AUC_m/AUC_p ratios were ≥ 0.25 for OH-OMP, OMP-S and C-OMP but not for DM-OMP. On the other hand, unbound AUC_m/AUC_p ratios were ≥ 0.25 for OH-OMP,

DMD Fast Forward. Published on April 25, 2013 as DOI: 10.1124/dmd.113.051722
This article has not been copyedited and formatted. The final version may differ from this version.

DM-OMP and C-OMP but not OMP-S, demonstrating a discrepancy between the two criteria. In addition, DM-OMP and OMP-S AUCs are likely < 10% of total drug related material as OMP-S was 10% and DM-OMP was 1% of the total quantified drug related material in this study. In the absence of radiolabelled data these values represent the upper limits of the abundance of the metabolites in relation to total drug related material. Since all four of the circulating metabolites were found to have exposures above 25% that of OMP when either the total or unbound AUCs were considered (Table 1), they were all evaluated for in vitro inhibitory potential and included in in vivo risk assessment. However, it is unclear whether DM-OMP would be considered if OMP was a drug under development as DM-OMP is a quantitatively minor metabolite.

CLog*P* values of OMP and its metabolites were calculated and the values are listed in Table 1. With the exception of OMP-S, all metabolites were less lipophilic than OMP. When the log*P* values were compared to the $f_{u,p}$ for each compound, overall increased Clog*P* values were associated with increased plasma protein binding (decreased fraction unbound in plasma) with the exception of DM-OMP, which has a higher Clog*P* than either OH-OMP or C-OMP but is less bound to plasma proteins (Table 1).

***In vitro* Inhibition of CYP2C19 and CYP3A4 by Omeprazole and Its Metabolites:** Reversible and irreversible inhibition of CYP2C19 and CYP3A4 by OMP and its metabolites was evaluated in pooled HLMs that were genotyped to be CYP2C19 extensive metabolizers and lack CYP3A5 expression. HLMs were selected as CYP2C19 extensive metabolizers for consistency and to obtain data not confounded by genetic variation in CYP2C19 expression levels. Similarly HLMs genotyped as CYP3A5 expressers were excluded since differentiation between CYP3A4 and CYP3A5 activity via selective substrates is not possible, and inactivation kinetics and inhibitory

DMD Fast Forward. Published on April 25, 2013 as DOI: 10.1124/dmd.113.051722
This article has not been copyedited and formatted. The final version may differ from this version.

potency of omeprazole may be different between CYP3A4 and CYP3A5. OMP was found to be a more potent inhibitor of CYP2C19-catalyzed (S)-mephenytoin metabolism (IC_{50} value of 8.4 ± 0.6 μM) than CYP3A4 catalyzed midazolam hydroxylation (IC_{50} value of 40 ± 4 μM) (Supplemental Fig. S1 and Table 2). All four metabolites (OH-OMP, DM-OMP, OMP-S and C-OMP) also inhibited CYP2C19 and CYP3A4 reversibly, with OMP-S being the most potent inhibitor based on the reversible IC_{50} values (Supplemental Fig. S2 and Table 2). Interestingly, based on the IC_{50} values, all of the metabolites except C-OMP were more potent CYP3A4 inhibitors than OMP. OMP-S was a more potent CYP2C19 inhibitor than the other metabolites (Table 2). While C-OMP also inhibited CYP2C19 and CYP3A4, the IC_{50} value for CYP2C19 could not be accurately determined due to lack of solubility of C-OMP (Supplemental Fig. S2 and Table 2).

When IC_{50}-shift experiments were performed, a 10-fold NADPH-dependent shift for CYP2C19 and 1.5-fold IC_{50}-shift for CYP3A4 were observed with OMP, suggesting irreversible inhibition of CYP2C19 and CYP3A4 by OMP (Fig. 2 and Supplemental Table S1). Of the OMP metabolites, DM-OMP and OMP-S caused a ≥ 1.5-fold IC_{50}-shift (7.3- and 2.1-fold respectively) with CYP2C19 and DM-OMP also caused an IC_{50}-shift (2.0-fold) with CYP3A4 (Supplemental Table S1), suggesting that DM-OMP and OMP-S may contribute to the inactivation of CYP2C19, and DM-OMP may contribute to CYP3A4 inactivation. No significant IC_{50}-shift (< 1.5-fold shift) was observed with either OH-OMP or C-OMP in the presence of NADPH with CYP2C19 or CYP3A4, suggesting that OH-OMP and C-OMP do not inactivate CYP2C19 or CYP3A4 (Supplemental Fig. S3 and Supplemental Table S1).

To characterize the irreversible inhibition of CYP2C19 and CYP3A4 by OMP and its metabolites, the K_I and k_{inact} values were determined for OMP and those metabolites that showed

DMD Fast Forward. Published on April 25, 2013 as DOI: 10.1124/dmd.113.051722
This article has not been copyedited and formatted. The final version may differ from this version.

a significant IC_{50}-shift. In agreement with the IC_{50}-shift experiments, time- and concentration-dependent inactivation of CYP2C19 was observed with OMP, DM-OMP and OMP-S (Fig. 3). All three compounds (OMP, OMP-S and DM-OMP) showed similar inactivation kinetics towards CYP2C19 with K_I values between 5 and 9 μM and k_{inact} values between 0.015 and 0.03 min^{-1} (Table 2). Of the three CYP2C19 inactivators, OMP appeared to be most efficient based on the k_{inact}/K_I ratios. Time- and concentration-dependent inactivation of CYP3A4 was also observed with OMP and DM-OMP, as predicted from the IC_{50}-shift experiments (Fig. 4). OMP and DM-OMP were less potent inactivators of CYP3A4 than CYP2C19 based on the fact that their K_I values were 7-10 fold higher towards CYP3A4. Yet, the k_{inact} value for OMP was similar towards both CYP3A4 and CYP2C19 while DM-OMP had a slightly higher (4.3-fold) k_{inact} value towards CYP3A4 than towards CYP2C19 (Table 2). In contrast to the rank order of inhibition efficiency between the compounds with CYP2C19, DM-OMP was a more efficient irreversible inhibitor of CYP3A4 than OMP based on the 3-fold higher k_{inact}/K_I ratio.

To assess whether CYP2C19-mediated formation of the DM-OMP is required for the irreversible inhibition of CYP3A4 by OMP in HLMs, inactivation of CYP3A4 by OMP was further evaluated using CYP3A4 supersomes. As shown in Fig. 4, irreversible inhibition of CYP3A4 by OMP was observed in the absence of CYP2C19 and OMP had a higher K_I (157 μM) and k_{inact} (0.054 min^{-1}) towards CYP3A4 in supersomes when compared to HLMs. The inactivation efficiency in supersomes was slightly lower than in HLMs, based on the k_{inact}/K_I ratio.

The Clog*P*'s of OMP and its metabolites were compared to the IC_{50} values and k_{inact}/K_I ratios to assess whether lipophilicity was predictive of the inhibition potency (Tables 1 and 2). A

DMD Fast Forward. Published on April 25, 2013 as DOI: 10.1124/dmd.113.051722
This article has not been copyedited and formatted. The final version may differ from this version.

correlation analysis was not possible due to the small sample size. However, for CYP2C19, reversible inhibition potency appears to be higher for more lipophilic compounds. For CYP3A4, the ClogP rank order did not predict the rank order of inhibitory potency of the metabolites. To determine that the rank order of inhibitory potency and ClogP was not confounded by protein binding issues the unbound fractions of OMP and its metabolites were determined in HLMs at the protein concentrations used for reversible and irreversible inhibition experiments and are shown in Table 2. The nonspecific binding of OMP and its metabolites was insignificant at both HLM protein concentrations.

Contribution of Omeprazole and Its Metabolites to DDI Risk Assessment: Using the in vitro inhibitory parameters and in vivo concentrations of OMP, OH-OMP, DM-OMP, OMP-S and C-OMP following the 20 mg single oral dose, the DDI risk and metabolite contribution to DDI risk assessment was evaluated. First, the DDI risk was predicted based on reversible [I]/K_i ratios for CYP2C19 and CYP3A4 (Table 3). While a CYP2C19- or CYP3A4-mediated DDI risk was not identified based on reversible [I]/K_i ratios of OMP with total and unbound C_{max} values, inclusion of all the metabolites with total C_{max} values did indicate a CYP2C19-mediated DDI risk as the sum of the [I]/K_i ratios was > 0.1 when total C_{max} value was used. However, using the 0.02 cutoff with unbound C_{max} value did not identify DDI risk. The CYP3A4-mediated DDI risk was missed both with total and unbound C_{max} values even when metabolites and gut inhibition were included in the risk assessment (Table 3).

Identification of OMP as an irreversible inhibitor of both CYP2C19 and CYP3A4 was critical for appropriate risk assessment of in vivo DDIs. The λ/k_{deg} value for OMP was > 0.1 and 0.25 with CYP2C19 using total or unbound C_{max} values, respectively, and inclusion of the metabolites increased the overall DDI risk (Table 3). With CYP3A4, the λ/k_{deg} value for OMP

DMD Fast Forward. Published on April 25, 2013 as DOI: 10.1124/dmd.113.051722
This article has not been copyedited and formatted. The final version may differ from this version.

identified the DDI risk when total C_{max} value was used or gut inhibition was considered. Using unbound C_{max} values, a hepatic CYP3A4 inhibition risk was only detected using the λ/k_{deg} cutoff of 0.1 and when DM-OMP was included in the risk assessment (Table 3). The unbound $\sum\lambda/k_{deg}$ does not exceed 0.25, which is the EMA cutoff. Overall, using the conservative λ/k_{deg} cutoff of 0.1 and total C_{max} value the DDI risk following OMP administration was identified without additional consideration of the metabolites.

For reversible CYP2C19 inhibition, the contribution of the metabolites was predicted to be up to 47% of the total interaction risk (Fig. 5 and Supplemental Fig. S4). However, the inhibition of CYP2C19 following OMP administration was determined to be mainly due to the inactivation of CYP2C19 by OMP and/or its metabolites. Hence, the metabolites were predicted to contribute up to 33% of CYP2C19 inhibition based on unbound concentrations. In contrast, with CYP3A4, based on unbound concentrations, metabolites contribute 88 % of the total hepatic CYP3A4 inhibition risk when reversible inhibition is considered, and up to 63% when irreversible inhibition is considered (Fig. 5, and Table 3). The percent contributions of metabolites based on their total concentrations are shown in Supplemental Fig. S4. These risk assessments do not consider intestinal CYP3A4 inhibition by systemic metabolites as it is unclear how intestinal inhibition by systemically formed metabolites should be assessed in DDI risk analysis and whether circulating metabolite concentrations can be used to predict intestinal inhibition of P450s. Regardless, the contribution of metabolites was different for the two P450s inhibited. In addition the minor metabolite of the quantified metabolites, DM-OMP, was the most relevant in DDI risk assessment.

Discussion

Testing of P450 inhibition by metabolites is recommended by the FDA and EMA. This may identify inhibition potential not possessed by the parent drug, aid in predictions of in vivo DDI magnitude and in modeling the time-course of the DDI. However, only a few studies have been conducted to evaluate the relative importance and modeling of metabolites in in vivo DDIs (Templeton et al., 2008; Rowland-Yeo et al 2010; VandenBrink and Isoherranen, 2010; Yeung et al., 2011; Reese et al 2008; Zhang et al., 2009). It is unclear whether the relative exposures of metabolites generally correlate with their importance in DDIs. For example, with the CYP3A4 inhibitor itraconazole, the minor metabolite N-desalkyl-itraconazole is predicted to have similar importance in in vivo DDIs as the major metabolite hydroxy-itraconazole (Templeton et al., 2008). Similarly with the CYP2D6 inhibitor bupropion, erythrobupropion is predicted to have similar role in in vivo DDIs as hydroxybupropion despite its 10-fold lower circulating concentrations (Yeung et al., 2011). To partially address this apparent discrepancy between metabolite exposure and importance in DDIs, consideration of the log*P* of metabolites was recently recommended for decision-trees regarding testing of specific metabolites for inhibition (Yu et al., 2012). In addition, it was suggested that for drugs that have structural alerts for MBI, such as alkyamines and epoxides, metabolites should be tested regardless of their exposure (Yu et al., 2012). However, many compounds, such as omeprazole, are MBIs but do not have obvious structural alerts to trigger DDI evaluation. The aim of this study was to determine, using OMP as an example, whether circulating total or unbound metabolite concentrations could be used to guide in vitro metabolite testing strategy, and whether metabolite contribution will aid in predicting in vivo DDIs.

In this study circulating metabolites of OMP were characterized. As a conservative

approach, quantified metabolites were evaluated in vitro if they met any of the criteria for circulating metabolites described by the FDA or EMA. However, DM-OMP only meets the criteria of >25% of the parent using unbound concentrations and it is <10% of total drug related material. As such it is unclear if testing of this quantitatively minor metabolite would be considered necessary. Furthermore, the EMA guidance may not require testing of any of these metabolites. Overall the analysis of in vivo AUC_m/AUC_p ratios determined for OMP and its metabolites demonstrates the discrepancies and ambiguity of decision making for metabolite testing. When metabolite evaluation is based solely based on metabolite exposure, DM-OMP is the metabolite that would likely be omitted. However, this was the only metabolite that is expected to contribute to in vivo DDIs with CYP2C19 and CYP3A4 and evaluation of OH-OMP, OMP-S and C-OMP could be considered unnecessary. Hence, it is important to further develop cutoffs for metabolite testing and ensure that the metabolites that are important in DDIs are tested.

Prioritization of metabolite testing based on the lipophilicity of the metabolites has been suggested so that metabolites that are less lipophilic than the parent drug should circulate at concentrations >100% of the parent to warrant testing for reversible inhibition (Yu et al., 2012). In the present study, all of the metabolites were estimated to be less lipophilic than OMP, except for OMP-S. As such, if metabolite lipophilicity is considered, OMP-S would warrant attention. However, its contribution to the overall DDI risk was predicted to be minimal (5-8% when unbound C_{max} is used) so testing of OMP-S could be considered unnecessary. With consideration of lipophilicity, DM-OMP would not be studied unless it was flagged for MBI.

Identification of OMP as an MBI is the key element in evaluating DDI risk. OMP is a well-characterized in vivo CYP2C19 inhibitor. It increases the AUC of moclobemide, a

DMD Fast Forward. Published on April 25, 2013 as DOI: 10.1124/dmd.113.051722
This article has not been copyedited and formatted. The final version may differ from this version.

CYP2C19 probe, by 120% (Yu et al., 2001), the AUC of proguanil by 50% (Funck-Brentano et al., 1997), the AUC of diazepam by 25% (Ishizaki et al 1995) and decreases the formation of the active metabolite of clopidogrel (Angiolillo et al., 2011). OMP also appears to inhibit CYP3A4 in vivo based on a 25% increase in nifedipine AUC (Soons et al., 1991) and 90% increase in carbamazepine AUC (Dixit et al., 2001) but studies with sensitive CYP3A4 probes have not been conducted. The results of this study suggest that better characterization of omeprazole as a CYP3A4 inhibitor is warranted. Consideration of reversible inhibition alone would not trigger CYP2C19 DDI studies unless all metabolites were considered together with OMP using total C_{max} values. However, wwhen OMP is recognized as an MBI of CYP2C19 the predicted in vivo λ/k_{deg} values were > 0.1 using total and > 0.25 using unbound C_{max} values. Inclusion of the metabolites increased the estimated DDI risk only slightly, and the metabolites were predicted to contribute 20-50% of the estimated CYP2C19 DDIs. This may be important if more sophisticated prediction methods such as PBPK models are employed. With CYP3A4, use of total OMP C_{max} values for the worst-case scenario risk assessment may provide a sufficient safety margin to ignore metabolite contribution during risk assessment as long as MBI is considered. Total C_{max} values usually overpredict in vivo DDIs while unbound C_{max} values are more predictive of in vivo interactions (Obach et al., 2007; Fujioka et al., 2012). Hence, with OMP, the conservative approach of using total C_{max} values would likely provide adequate data to trigger in vivo studies without consideration of metabolites.

To our knowledge, irreversible inhibition of CYP3A4 by OMP and the inactivation kinetics of CYP2C19 and CYP3A4 by OMP metabolites have not been previously characterized. The inactivation kinetics of CYP2C19 by OMP has been reported and the DDI between clopidogrel and OMP has been predicted using OMP data alone (Ogilvie et al., 2011; Boulenc et al., 2012).

DMD Fast Forward. Published on April 25, 2013 as DOI: 10.1124/dmd.113.051722
This article has not been copyedited and formatted. The final version may differ from this version.

In addition, OMP-S was previously shown to cause an IC_{50}-shift in vitro with CYP2C19, and the inactivation of CYP2C19 by OMP was proposed to involve DM-OMP (Ogilvie et al., 2011). Our studies demonstrate that DM-OMP is an inactivator of CYP2C19, and it is possible that the proposed mechanisms in which a reactive quinoneimine is formed after 5'-O-demethylation by CYP2C19 is responsible for CYP2C19 inactivation (Ogilvie et al., 2011). However, if quinoneimine formation from DM-OMP is required for CYP2C19 inactivation, it is surprising that the k_{inact} value was the highest for OMP in comparison to OMP-S and DM-OMP. It is unclear how inactivation proceeds from OMP-S, which has not been shown to undergo O-demethylation. Further studies are required to determine the mechanism of CYP2C19 inactivation by OMP. The reactive quinoneimine formation by CYP3A4 may be responsible for CYP3A4 inactivation as the inactivation rate was faster from DM-OMP than OMP and OMP-S did not result in CYP3A4 inactivation. While the DM-OMP formation is generally believed to be by CYP2C19 (Andersson and Weidolf, 2008), the data in CYP3A4 supersomes shows that CYP3A4 inactivation does not require CYP2C19. This suggests that either CYP3A4 forms sufficient quantities of DM-OMP that is not released from CYP3A4 active site and results in CYP3A4 inactivation, or that the quinoneimine is not responsible for CYP3A4 inactivation. The qualitative differences between CYP2C19 and CYP3A4 inactivation by OMP and its metabolites are of interest as they demonstrate that P450 inactivation mechanisms and relative metabolite contributions cannot be easily generalized and extrapolated. The data also show that metabolites formed by one P450 (DM-OMP by CYP2C19 and OMP-S by CYP3A4) may be relevant in inhibition of other P450s.

OMP has a short half-life and its metabolites, with the exception of OMP-S, follow formation rate limited kinetics. Due to its short half-life, use of time-varying DDI models may

be beneficial for quantitative DDI predictions of OMP. The risk predictions provided here should not be directly used for quantitative DDI predictions. However, the metabolite to parent concentration ratio does not change as a function of time for OH-OMP, DM-OMP and C-OMP, so the C_{max} ratios should provide a reasonable assessment of the relative importance of these metabolites in CYP2C19 and CYP3A4 inhibition. These predictions were made based on plasma concentrations in CYP2C19 extensive metabolizers after a 20 mg dose of OMP in a four drug cocktail. Since OMP inactivates CYP2C19, the metabolite ratios may change with increasing doses and multiple dosing, and better characterization of metabolite disposition following different dosing regimens is required for PBPK models of OMP. In addition, since OH-OMP DM-OMP and C-OMP are also reversible inhibitors of CYP2C19 and CYP3A4 and their $[I]/K_i$ ratios were, in many cases, higher than those for OMP it may be necessary to account for the inhibitor-inhibitor interactions between the metabolites and OMP in quantitative DDI predictions. Further work is required to develop the kinetic theory for multiple inactivators according to the theory provided for alkylamines (Zhang et al., 2009a, 2009b).

In conclusion, the results of this study show that identification of MBIs during drug development is critically important for DDI risk assessment. Based on the obtained data, DM-OMP is responsible for the majority of hepatic CYP3A4 inhibition while metabolites are responsible for <50% of the overall CYP2C19 inhibition. While metabolites may contribute to in vivo DDIs, their importance may not be related to their relative abundance in plasma. As such, better models need to be developed to prioritize metabolite testing in DDI assessment.

Authorship contributions:

Participated in research design: Shirasaka, Sager, Isoherranen, Lutz

Conducted experiments: Shirasaka, Sager, Lutz

Performed data analysis: Shirasaka, Sager, Lutz, Davis

Wrote or contributed to the writing of the manuscript: Shirasaka, Sager, Lutz, Isoherranen

References

Andersson T, Miners JO, Veronese ME, and Birkett DJ (1994) Identification of human liver cytochrome P450 isoforms mediating secondary omeprazole metabolism. *Br J Clin Pharmacol* **37:**597-604.

Andersson T and Weidolf L (2008) Stereoselective disposition of proton pump inhibitors. *Clin Drug Investig* **28**:263–279.

Angiolillo DJ, Gibson CM, Cheng S, Ollier C, Nicolas O, Bergougnan L, Perrin L, LaCreta FP, Hurbin F, and Dubar M (2011) Differential effects of omeprazole and pantoprazole on the pharmacodynamics and pharmacokinetics of clopidogrel in healthy subjects: randomized, placebo-controlled, crossover comparison studies. *Clin Pharmacol Ther* **89**:65-74.

Berry LM and Zhao Z (2008) An examination of IC50 and IC50-shift experiments in assessing time-dependent inhibition of CYP3A4, CYP2D6, and CYP2C9 in human liver microsomes. *Drug Metab Lett* **2**:51–59.

Boulenc X, Djebli N, Shi J, Perrin L, Brian W, Van Horn R, and Hurbin F (2012) Effects of omeprazole and genetic polymorphism of CYP2C19 on the clopidogrel active metabolite. *Drug Metab Dispos* **40**:187-197.

Brown LM and Ford-Hutchinson AW (1982) The destruction of cytochrome P-450 by alclofenac: possible involvement of an epoxide metabolite. *Biochem Pharmacol* **31:**195-199.

Dixit RK, Chawla AB, Kumar N, Garg SK (2001) Effect of omeprazole on the pharmacokinetics of sustained-release carbamazepine in healthy male volunteers. Methods Find Exp Clin Pharmacol **23**:37-39.

Fahmi OA, Boldt S, Kish M, Obach RS, and Tremaine LM (2008) Prediction of drug-drug interactions from in vitro induction data: application of the relative induction score

approach using cryopreserved human hepatocytes. *Drug Metab Dispos* **36:**1971-1974.

Fujioka Y, Kunze KL, and Isoherranen N (2012) Risk assessment of mechanism-based inactivation in drug-drug interactions. *Drug Metab Dispos* **40:**1653-1657.

Funck-Brentano C, Becquemont L, Lenevu A, Roux A, Jaillon P, and Beaune P (1997) Inhibition by omeprazole of proguanil metabolism: mechanism of the interaction in vitro and prediction of in vivo results from the in vitro experiments. *J Pharmacol Exp Ther* **280**:730-738.

Furuta S, Kamada E, Suzuki T, Sugimoto T, Kawabata Y, Shinozaki Y, and Sano H (2001) Inhibition of drug metabolism in human liver microsomes by nizatidine, cimetidine and omeprazole. *Xenobiotica* **31:**1-10.

Grimm SW, Einolf HJ, Hall SD, He K, Lim H-K, Ling KJ, Lu C, Nomeir AA, Seibert E, Skordos KW, Tonn GR, Van Horn R, Wang RW, Wong YN, Yang TJ, and Obach RS (2009) The conduct of in vitro studies to address time-dependent inhibition of drug-metabolizing enzymes: a perspective of the Pharmaceutical Research and Manufacturers of America. *Drug Metab Dispos* **37**:1355-1370.

Hassan-Alin M, Andersson T, Niazi M, and Rohss K (2005) A pharmacokinetic study comparing single and repeated oral doses of 20 mg and 40 mg omeprazole and its two optical isomers, S-omeprazole (esomeprazole) and R-omeprazole, in healthy subjects. *Eur J Clin Pharmacol* **60:**779-784.

Ishizaki T, Chiba K, Manabe K, Koyama E, Hayashi M, Yasuda S, Horai Y, Tomono Y, Yamato C, and Toyoki T (1995) Comparison of the interaction potential of a new proton pump inhibitor, E3810, versus omeprazole with diazepam in extensive and poor metabolizers of S-mephenytoin 4'-hydroxylation. *Clin Pharmacol Ther* **58**:155-164.

Isoherranen N, Hachad H, Yeung CK, and Levy RH (2009) Qualitative analysis of the role of metabolites in inhibitory drug-drug interactions: literature evaluation based on the metabolism and transport drug interaction database. *Chem Res Toxicol* **22:**294-298.

Li XQ, Andersson TB, Ahlstrom M, and Weidolf L (2004) Comparison of inhibitory effects of the proton pump-inhibiting drugs omeprazole, esomeprazole, lansoprazole, pantoprazole, and rabeprazole on human cytochrome P450 activities. *Drug Metab Dispos* **32:**821-827.

Lutz JD and Isoherranen N (2012) Prediction of relative in vivo metabolite exposure from in vitro data using two model drugs: dextromethorphan and omeprazole. *Drug Metab Dispos* **40**:159-168.

Nishiya Y, Hagihara K, Kurihara A, Okudaira N, Farid NA, Okazaki O, and Ikeda T (2009) Comparison of mechanism-based inhibition of human cytochrome P450 2C19 by ticlopidine, clopidogrel, and prasugrel. *Xenobiotica* **39:**836-843.

Obach RS, Walsky RL, and Venkatakrishnan K (2007) Mechanism-based inactivation of human cytochrome p450 enzymes and the prediction of drug-drug interactions. *Drug Metab Dispos* **35:**246-255.

Ogilvie BW, Yerino P, Kazmi F, Buckley DB, Rostami-Hodjegan A, Paris BL, Toren P, and Parkinson A (2011) The proton pump inhibitor, omeprazole, but not lansoprazole or pantoprazole, is a metabolism-dependent inhibitor of CYP2C19: implications for coadministration with clopidogrel. *Drug Metab Dispos* **39:**2020-2033.

Overton ET, Tschampa JM, Klebert M, Royal M, Rodriguez M, Spitz T, Kim G, Mondy KE and Acosta EP (2010) The effect of acid reduction with a proton pump inhibitor on the pharmacokinetics of lopinavir or ritonavir in HIV-infected patients on lopinavir/ritonavir-based therapy. *J Clin Pharmacol* **50:**1050-1055.

Reese MJ, Wurm RM, Muir KT, Generaux GT, John-Williams LS, and McConn DJ (2008) An in vitro mechanistic study to elucidate the desipramine/bupropion clinical drug-drug interaction. *Drug Metab Dispos* **36:**1198-1201.

Regårdh CG, Andersson T, Lagerström PO, Lundborg P, and Skånberg I (1990) The pharmacokinetics of omeprazole in humans--a study of single intravenous and oral doses. *Ther Drug Monit* **12**:163-172.

Rowland Yeo K, Jamei M, Yang J, Tucker GT, and Rostami-Hodjegan A (2010) Physiologically based mechanistic modeling to predict complex drug-drug interactions involving simultaneous competitive and time-dependent enzyme inhibition by parent compound and its metabolite in both liver and gut- The effect of diltiazem on the time-course of exposure to triazolam. *Eur J Pharm Sci* **39:**298-309.

Ryu, J. Y., I. S. Song, et al. (2007) Development of the "Inje cocktail" for high-throughput evaluation of five human cytochrome P450 isoforms in vivo. *Clin Pharmacol Ther* **82**(5): 531-40.

Singh K, Dickinson L, Chaikan A, Back D, Fletcher C, Pozniak A, Moyle G, Nelson M, Gazzard B, Herath D, and Boffito M (2008) Pharmacokinetics and safety of saquinavir/ritonavir and omeprazole in HIV-infected subjects. *Clin Pharmacol Ther* **83:**867-872.

Soons PA, van den Berg G, Danhof M, van Brummelen P, Jansen JB, Lamers CB, and Breimer DD (1992) Influence of single- and multiple-dose omeprazole treatment on nifedipine pharmacokinetics and effects in healthy subjects. *Eur J Clin Pharmacol* **42:**319-324.

Templeton IE, Thummel KE, Kharasch ED, Kunze KL, Hoffer C, Nelson WL, and Isoherranen N (2008) Contribution of itraconazole metabolites to inhibition of CYP3A4 in vivo. *Clin*

Pharmacol Ther **83**:77–85.

Uno T, Sugimoto K, Sugawara K, and Tateishi T (2008) The role of cytochrome P2C19 in R-warfarin pharmacokinetics and its interaction with omeprazole. *Ther Drug Monit* **30**:276-281.

VandenBranden M, Ring BJ, Binkley SN, and Wrighton SA (1996) Interaction of human liver cytochromes P450 in vitro with LY307640, a gastric proton pump inhibitor. *Pharmacogenetics* **6:**81-91.

VandenBrink BM and Isoherranen N (2010) The role of metabolites in predicting drug-drug interactions: focus on irreversible cytochrome P450 inhibition. *Curr Opin Drug Discov Devel* **13:**66-77.

Waley SG (1985) Kinetics of suicide substrates. Practical procedures for determining parameters. *Biochem J* **227:**843-849.

Yeung CK, Fujioka Y, Hachad H, Levy RH, and Isoherranen N (2011) Are circulating metabolites important in drug-drug interactions?: Quantitative analysis of risk prediction and inhibitory potency. *Clin Pharmacol Ther* **89:**105-113.

Yu H and Tweedie D (2012) A Perspective on the Possible Contribution of Metabolites to DDI Potential: The Need to Consider Both Circulating Levels and Inhibition Potency. *Drug Metab Dispos*.

Yu KS, Yim DS, Cho JY, Park SS, Park JY, Lee KH, Jang IJ, Yi SY, Bae KS, and Shin SG (2001) Effect of omeprazole on the pharmacokinetics of moclobemide according to the genetic polymorphism of CYP2C19. *Clin Pharmacol Ther* **69**:266-273.

Zhang X, Jones DR, and Hall SD (2009a) Prediction of the effect of erythromycin, diltiazem, and their metabolites, alone and in combination, on CYP3A4 inhibition. *Drug Metab Dispos*

37:150-160.

Zhang X, Quinney SK, Gorski JC, Jones DR, and Hall SD (2009b) Semiphysiologically based pharmacokinetic models for the inhibition of midazolam clearance by diltiazem and its major metabolite. *Drug Metab Dispos* **37**:1587-1597.

Zomorodi K and Houston JB (1996) Diazepam-omeprazole inhibition interaction: an in vitro investigation using human liver microsomes. *Br J Clin Pharmacol* **42:**157-162.

Zvyaga T, Chang SY, Chen C, Yang Z, Vuppugalla R, Hurley J, Thorndike D, Wagner A, Chimalakonda A, and Rodrigues AD (2012) Evaluation of six proton pump inhibitors as inhibitors of various human cytochromes P450: focus on cytochrome P450 2C19. *Drug Metab Dispos* **40:**1698-1711.

Footnotes

Yoshiyuki Shirasaka and Jennifer E. Sager contributed equally to this manuscript

This work was supported in part by grants from the National Institutes of Health P01 [GM32165] (J.D.L., CD., N.I.) and T32 [GM007750] (J.E.S). and (University of Washington Clinical Research Center). Research reported in this publication was supported in part by the National Center for Advancing Translational Sciences of the National Institutes of Health under Award Number UL1[TR000423]. The study was also supported in part by the Japan Society for the Promotion of Science Postdoctoral Fellowship for Research Abroad [H23-694] (Y.S) and a Grant-in-Aid for Scientific Research [21790147] (Y.S.).

Figure Legends

Figure 1. Mean plasma concentration-time profiles of omeprazole and its metabolites in nine healthy volunteers after oral administration of 20 mg omeprazole. Plasma concentrations of (A) Omeprazole, (B) 5-hydroxyomeprazole, (C) 5'-O-desmethylomeprazole, (D) omeprazole sulfone and (E) carboxyomeprazole were quantified. Data are shown as means ± S.D. (n = 9).

Figure 2. NADPH-dependent IC_{50}-shifts for omeprazole and its metabolites for CYP2C19-catalyzed (S)-mephenytoin hydroxylation and CYP3A4-catalyzed midazolam hydroxylation in HLMs. Inhibition of CYP2C19 and CYP3A4 by omeprazole (A and B), 5'-O-desmethylomeprazole (C and D) and omeprazole sulfone (E and F) is shown following a 30 minute pre-incubation with the inhibitor in the presence or absence of NADPH. All incubations were done as described in Materials and Methods. Data are shown as means ± S.D. (n = 3).

Figure 3. Inactivation kinetics of CYP2C19 by omeprazole (A), 5'-O-desmethylomeprazole (B) and omeprazole sulfone (C) in HLMs using (S)-mephenytoin hydroxylation as a probe. The left panels show the time-dependent inactivation of CYP2C19 at various concentrations of omeprazole and its metabolites. The right panels show the fit of equation 2 to the data. Data are shown as means ± S.D. (n = 3).

Figure 4. Inactivation kinetics of CYP3A4 by omeprazole in HLM (A) omeprazole in CYP3A4 supersomes (B) and 5'-O-desmethylomeprazole in HLMs (C). The left panels show the time-dependent inactivation of CYP3A4 at various concentrations of omeprazole and DM-OMP. The right panels show the fit of equation 2 to the data. Data are shown as means ± S.D. (n = 3).

DMD Fast Forward. Published on April 25, 2013 as DOI: 10.1124/dmd.113.051722
This article has not been copyedited and formatted. The final version may differ from this version.

Figure 5. Predicted relative contribution of omeprazole and its metabolites to reversible (I/IC_{50}) and irreversible (λ/k_{deg}) CYP2C19- and CYP3A4 inhibition. The inhibition risk was predicted using unbound C_{max} values.

Table 1. In Vivo Pharmacokinetic Parameters of Omeprazole and its Metabolites

Inhibitor	Clog *P*	C_{max} (μM)	$AUC_{0-\infty}$ (hr*nM)	$f_{u,p}$	AUC_m/AUC_p		AUC_m/AUC_t[a]
					Total $AUC_{0-\infty}$	Unbound $AUC_{0-\infty}$	Total $AUC_{0-\infty}$
OMP	2.23	0.66 ±0.34	1200 ±600	0.05± 0.02			
OH-OMP	0.98	0.48 ±0.33	1000 ±400	0.17 ± 0.03	0.83	2.7	≤ 0.27
DM-OMP	1.90	0.03 ±0.01	49 ±12	1.0 ± 0.1	0.04	0.79	≤ 0.01
OMP-S	2.24	0.14 ± 0.10	390 ±220	0.02 ± 0.004	0.33	0.14	≤ 0.10
C-OMP	1.39	0.25 ±0.10	1100 ±400	0.08 ± 0.02	0.92	1.4	≤ 0.29

$f_{u,p}$ is the fraction of omeprazole and metabolites unbound in plasma, AUC_m if the AUC of the metabolite, AUC_p is the AUC of the parent (OMP) and AUC_t is the summed AUC of all measured compounds. [a]In the absence of a mass-balance study, the maximum possible fraction of total drug related material was estimated as a fraction of all quantified compounds.

Table 2. In Vitro Inhibitory Parameters of Omeprazole and Metabolites for CYP2C19 and CYP3A4

Target P450	Inhibitor	*In vitro* Parameters					
		$f_{u,m(0.1)}$ [a]	$f_{u,m(1.0)}$ [a]	IC_{50} (μM)	K_I (μM)	k_{inact} (min^{-1})	k_{inact}/K_I ($L \cdot min^{-1} \cdot \mu mol^{-1}$)
CYP2C19	OMP	0.98 ± 0.06	0.92 ± 0.04	8.4 ± 0.6	8.2 ±3.6	0.029 ± 0.004	0.0035
	OH-OMP	0.95 ± 0.06	0.93 ± 0.05	39 ± 2	N.D.	N.D.	N.D.
	DM-OMP	1.0 ± 0.1	1.0 ± 0.1	31 ±2	8.7 ±4.3	0.020 ± 0.003	0.0022
	OMP-S	0.96 ± 0.02	0.89 ± 0.05	5.1 ±0.2	5.7 ± 0.8	0.015 ± 0.001	0.0026
	COMP	0.98 ± 0.05	0.98 ± 0.05	> 50	N.D.	N.D.	N.D.
CYP3A4	OMP	0.98 ± 0.06	0.92 ±0.04	40 ± 4	52 ±8	0.029 ± 0.001	0.0006
	OH-OMP	0.95 ± 0.06	0.93 ± 0.05	21 ± 4	N.D.	N.D.	N.D.
	DM-OMP	1.0 ± 0.1	1.0 ± 0.1	15 ± 4	61 ±15	0.086 ± .010	0.0014
	OMP-S	0.96 ± 0.02	0.89 ± 0.05	8 ± 1	N.D.	N.D.	N.D.
	COMP	0.98 ± 0.05	0.98 ± 0.05	48 ± 6	N.D.	N.D.	N.D.

[a] $f_{u,m(0.1)}$ and $f_{u,m(1.0)}$ are the microsomal unbound fractions of omeprazole and its metabolites for 0.1 mg/mL and 1.0 mg/mL HLMs, respectively. N.D., not determined. Data are shown as means ± S.D. (n = 3).

Table 3. Assessment of In Vivo CYP2C19 and CYP3A4 Inhibition Risk by Omeprazole and Metabolites

Target P450	Inhibitor	Reversible ([I]/K_i)[a]		Irreversible (λ/k_{deg})	
		C_{max}	$C_{max*}f_u$	C_{max}	$C_{max*}f_u$
CYP2C19 (hepatic)	OMP	0.080	0.0042	5.2	0.29
	OH-OMP	0.012	0.0022	N.D.	N.D.
	DM-OMP	0.0008	0.0008	0.12	0.12
	OMP-S	0.028	0.0007	0.92	0.022
	COMP	N.D.	N.D.	N.D.	N.D.
	Total	0.12	0.0078	6.25	0.44
CYP3A4 (hepatic)	OMP	0.017	0.0009	1.23	0.065
	OH-OMP	0.024	0.004	N.D.	N.D.
	DM-OMP	0.002	0.002	0.11	0.11
	OMP-S	0.017	0.0004	N.D.	N.D.
	COMP	0.005	0.0004	N.D.	N.D.
	Total	0.066	0.0074	1.34	0.18
CYP3A4 (intestinal)	OMP	6.0	6.0	50	50

[a][I]/K_i is extrapolated from the [I]/IC_{50} ratio. Since substrate concentration was <<K_m for all IC_{50} experiments the IC_{50} was assumed to be equivalent to K_i. [I]/IC_{50} and λ/k_{deg} values are calculated based on in vitro inhibitory parameters shown in Table 2. Either total or unbound C_{max} were used for inhibitor concentration. N.D., not detected.

Figure 1

DMD Fast Forward. Published on April 25, 2013 as DOI: 10.1124/dmd.113.051722
This article has not been copyedited and formatted. The final version may differ from this version.

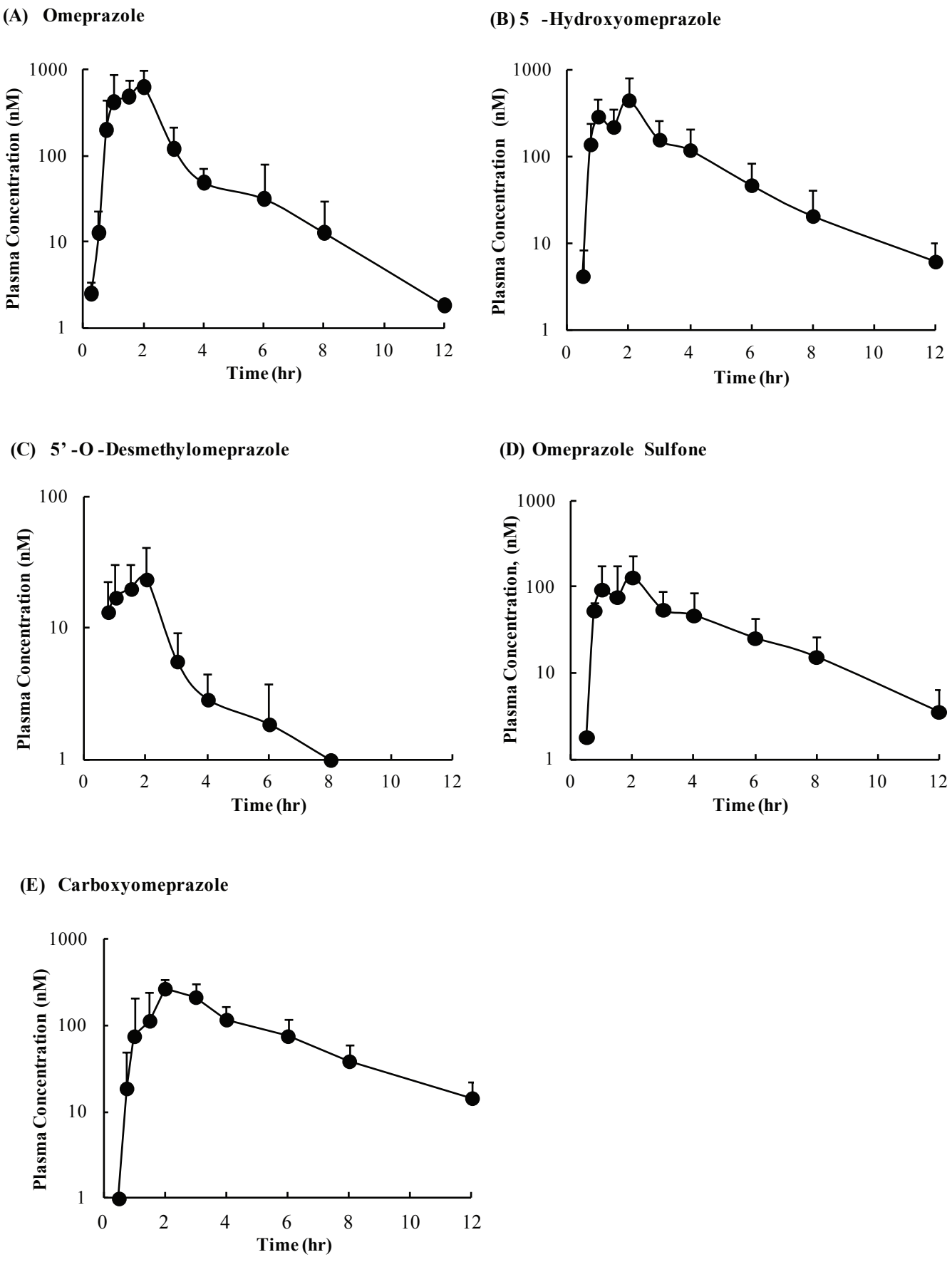

DMD Fast Forward. Published on April 25, 2013 as DOI: 10.1124/dmd.113.051722
This article has not been copyedited and formatted. The final version may differ from this version.

Figure 2

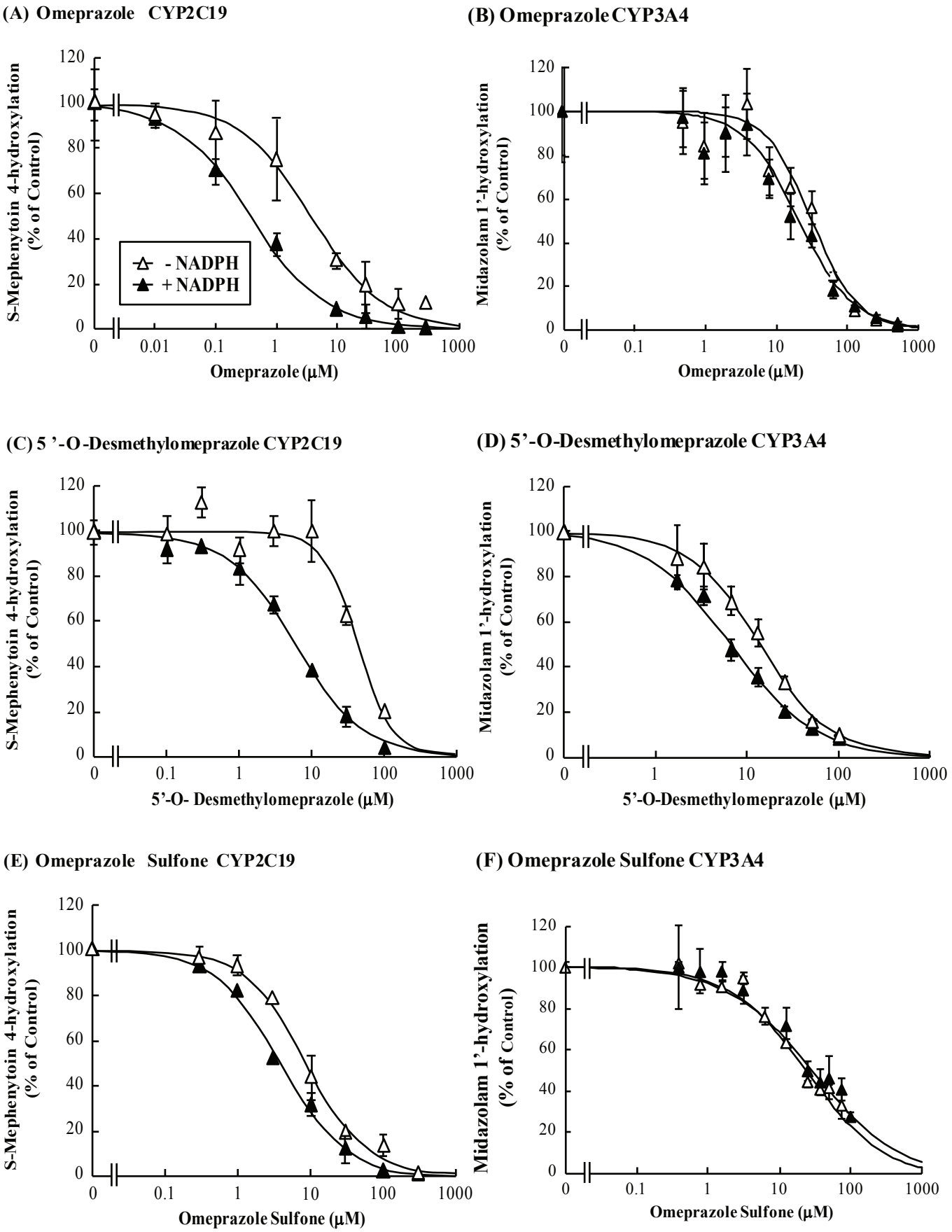

DMD Fast Forward. Published on April 25, 2013 as DOI: 10.1124/dmd.113.051722
This article has not been copyedited and formatted. The final version may differ from this version.

Figure 3

(A) Omeprazole

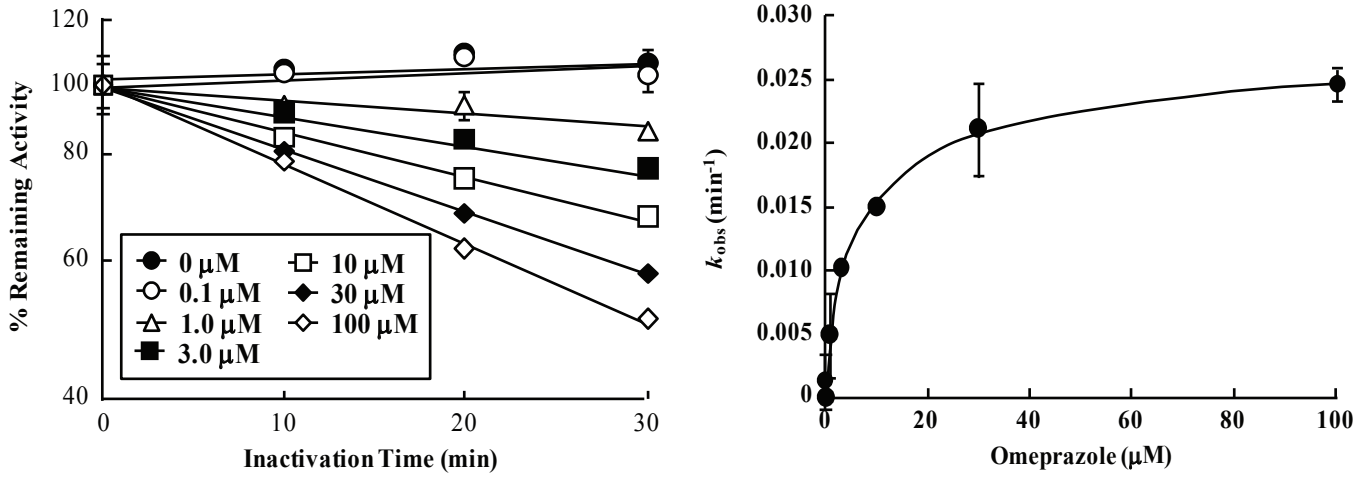

(B) 5' -O-Desmethylomeprazole

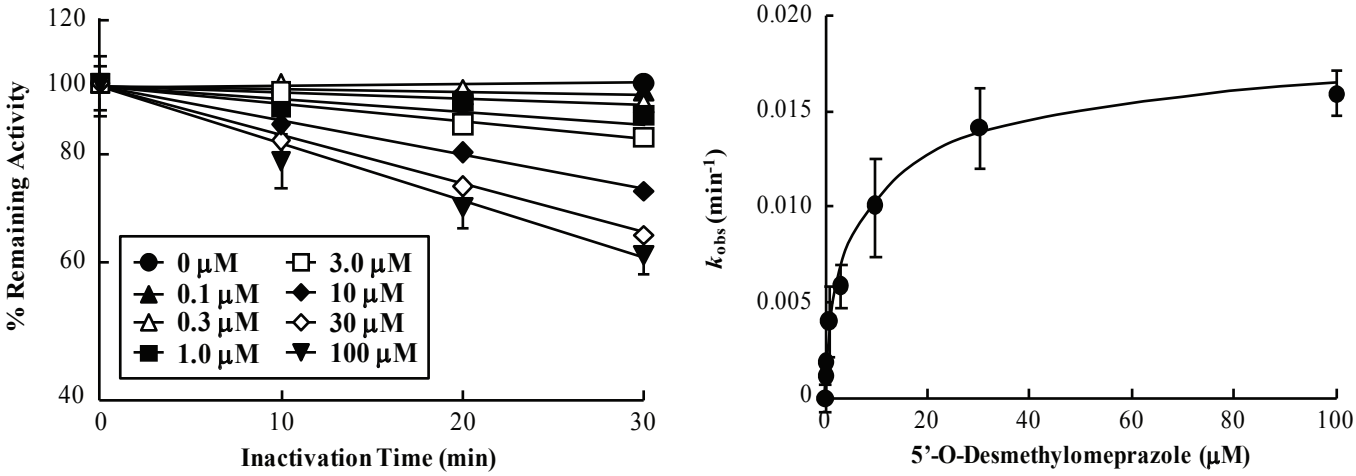

(C) Omeprazole Sulfone

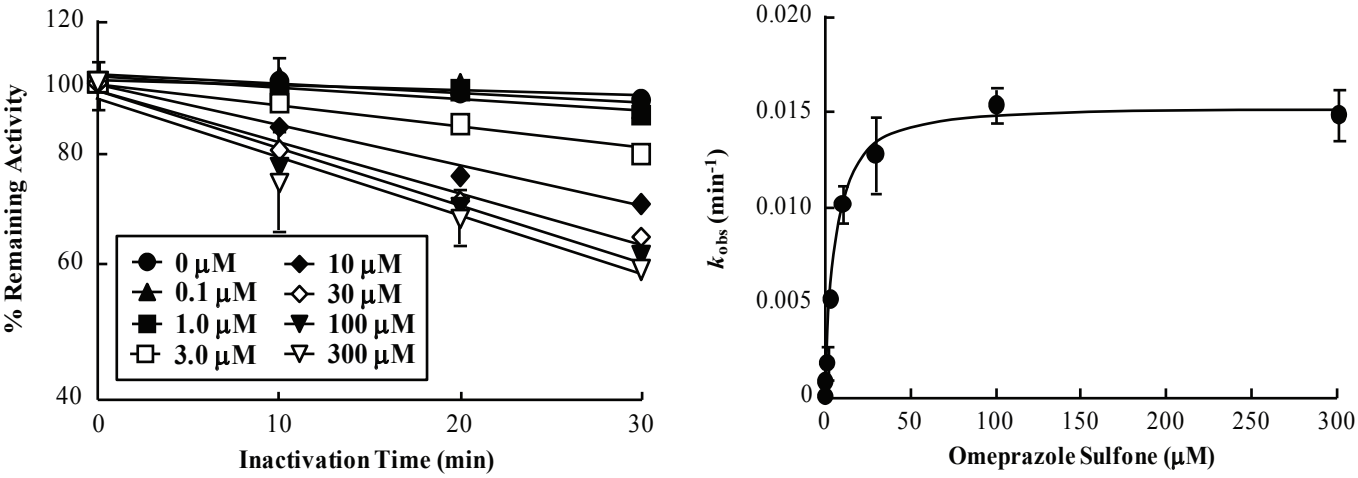

DMD Fast Forward. Published on April 25, 2013 as DOI: 10.1124/dmd.113.051722
This article has not been copyedited and formatted. The final version may differ from this version.

Figure 4

(A) Omeprazole in HLMs

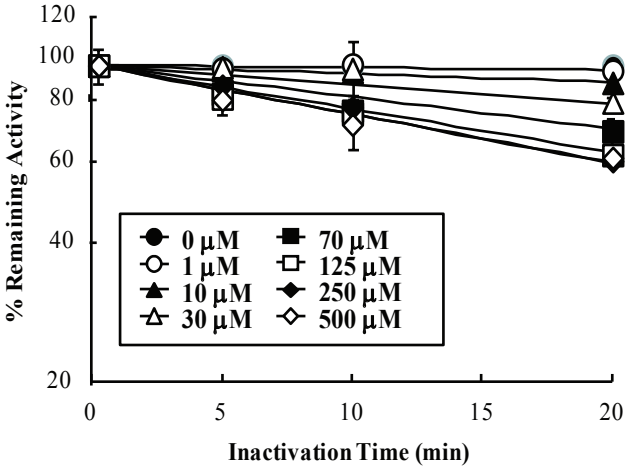

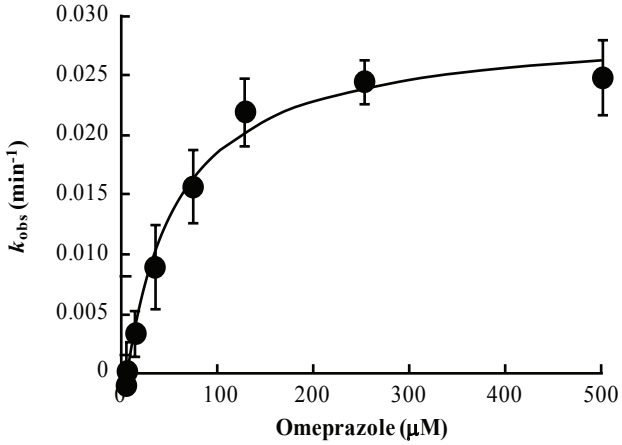

(B) Omeprazole in CYP3A4 Supersomes

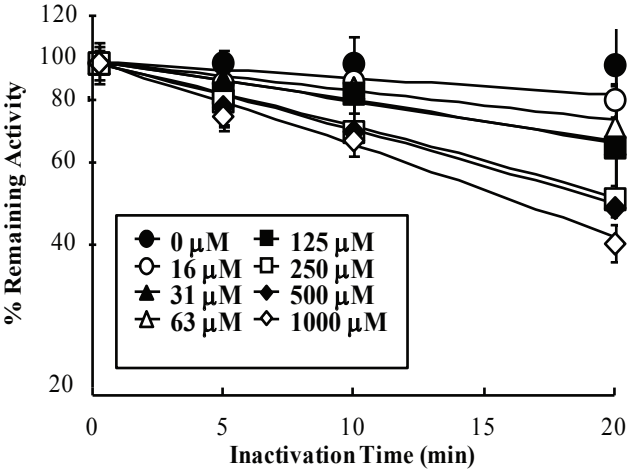

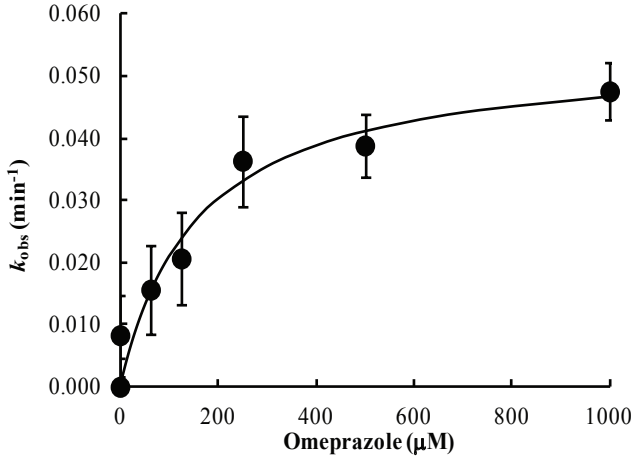

(C) 5'-O-Desmethylomeprazole in HLMs

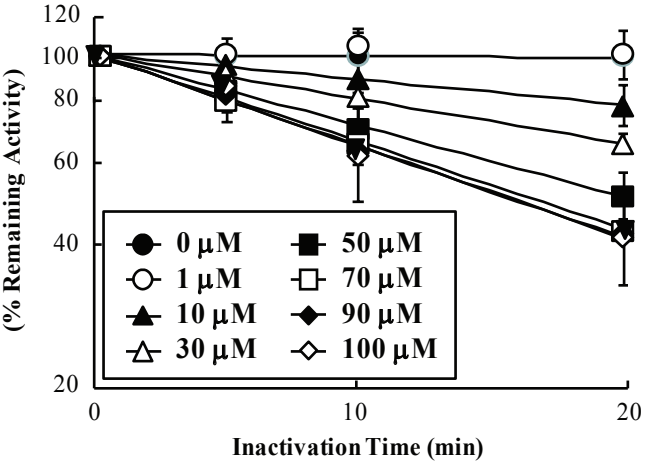

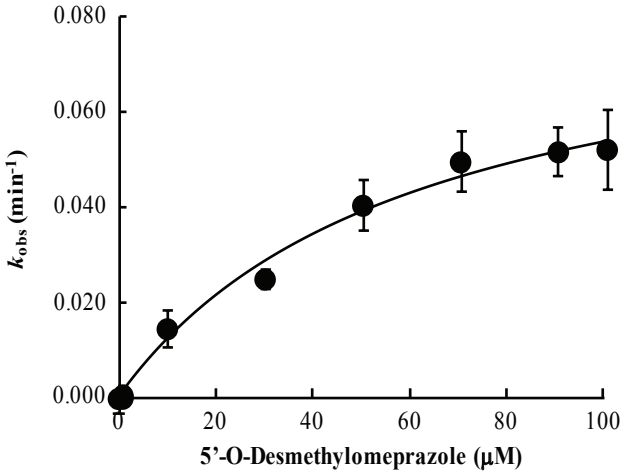

DMD Fast Forward. Published on April 25, 2013 as DOI: 10.1124/dmd.113.051722
This article has not been copyedited and formatted. The final version may differ from this version.

Figure 5

(A) Reversible Inhibition ($\sum[I]/K_i$)

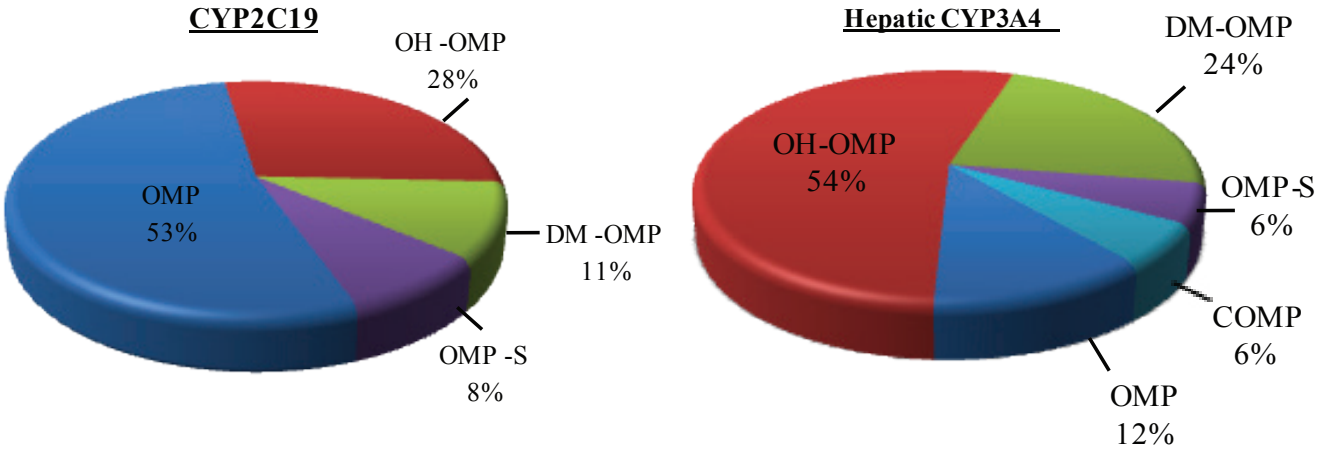

(B) Irreversible inhibition ($\sum\lambda / k_{deg}$)